The EMBO Journal (2009) 28, 1589–1600 | © 2009 European Molecular Biology Organization | All Rights Reserved 0261-4189/09
www.embojournal.org

THE EMBO JOURNAL

SLP-2 is required for stress-induced mitochondrial hyperfusion

Daniel Tondera[1,9,10], Stéphanie Grandemange[1,9,11], Alexis Jourdain[1], Mariusz Karbowski[2], Yves Mattenberger[1], Sébastien Herzig[1], Sandrine Da Cruz[1,12], Pascaline Clerc[3], Ines Raschke[4], Carsten Merkwirth[4], Sarah Ehses[4], Frank Krause[5], David C Chan[6], Christiane Alexander[7], Christoph Bauer[8], Richard Youle[3], Thomas Langer[4] and Jean-Claude Martinou[1,*]

[1]Department of Cell Biology, University of Geneva, Geneva, Switzerland, [2]Medical Biotechnology Center, University of Maryland Biotechnology Institute, Baltimore, MD, USA, [3]Biochemistry Section, Surgical Neurology Branch, National Institute of Neurological Disorders and Stroke, National Institutes of Health, Bethesda, MD, USA, [4]Institute for Genetics and Centre for Molecular Medicine (CMMC), University of Cologne, Cologne, Germany, [5]Physical Biochemistry, Department of Chemistry, Technische Universität Darmstadt, Darmstadt, Germany, [6]Division of Biology, California Institute of Technology, Pasadena, CA, USA, [7]Department of Neuroscience, Max-Delbrück-Center for Molecular Medicine, Berlin, Germany and [8]Imaging Platform, NCCR Frontiers in Genetics, University of Geneva, Geneva, Switzerland

Mitochondria are dynamic organelles, the morphology of which results from an equilibrium between two opposing processes, fusion and fission. Mitochondrial fusion relies on dynamin-related GTPases, the mitofusins (MFN1 and 2) in the outer mitochondrial membrane and OPA1 (optic atrophy 1) in the inner mitochondrial membrane. Apart from a role in the maintenance of mitochondrial DNA, little is known about the physiological role of mitochondrial fusion. Here we report that mitochondria hyperfuse and form a highly interconnected network in cells exposed to selective stresses. This process precedes mitochondrial fission when it is triggered by apoptotic stimuli such as UV irradiation or actinomycin D. Stress-induced mitochondrial hyperfusion (SIMH) is independent of MFN2, BAX/BAK, and prohibitins, but requires L-OPA1, MFN1, and the mitochondrial inner membrane protein SLP-2. In the absence of SLP-2, L-OPA1 is lost and SIMH is prevented. SIMH is accompanied by increased mitochondrial ATP production and represents a novel adaptive pro-survival response against stress.

*Corresponding author. Department of Cell Biology, University of Geneva, 30 quai Ernest-Ansermet, 4 Geneva 1211, Switzerland.
Tel.: +41 22 379 6443; Fax: +41 22 379 6442;
E-mail: Jean-Claude.Martinou@unige.ch
[9]These authors contributed equally to this work
[10]Present address: Dana-Farber Cancer Institute, Boston, MA, USA
[11]Present address: EA 4001 Predicther, Université Henri Poincaré-Nancy Université, Nancy, France
[12]Present address: Ludwig Institute for Cancer Research, University of California San Diego, La Jolla, CA, USA

Received: 24 November 2008; accepted: 12 March 2009; published online: 9 April 2009

The EMBO Journal (2009) **28,** 1589–1600. doi:10.1038/emboj.2009.89; Published online 9 April 2009
Subject Categories: differentiation & death; cellular metabolism
Keywords: ATP; fusion; mitochondria; stress; survival

Introduction

The morphology of mitochondria in eukaryotic cells is constantly shaped by the opposing processes of fission and fusion (Hoppins *et al*, 2007). This dynamic behaviour is essential for normal mitochondrial function and participates in fundamental processes, including development, apoptosis, and ageing (Chan, 2006). During the recent years, several key elements of the mitochondrial fission and fusion machinery have been identified, among which at least four dynamin-related GTPases, mitofusin 1 (MFN1), mitofusin 2 (MFN2), optic atrophy 1 (OPA1), and dynamin-related protein 1 (DRP1), play an essential role (Hoppins *et al*, 2007). MFN1 and 2 are located in the outer mitochondrial membrane and mediate outer membrane fusion by the formation of homo- and heterodimers that tether adjacent mitochondria (Koshiba *et al*, 2004). OPA1 is responsible for fusion of the inner mitochondrial membrane, and exerts an effect in concert with MFN1 to coordinate fusion of the two membranes (Cipolat *et al*, 2004). In addition, OPA1, through the formation of oligomers, has a function in the formation of the cristae junction (Frezza *et al*, 2006). Finally, DRP1 is required for the fission of the outer mitochondrial membrane (Smirnova *et al*, 2001).

Mitochondrial fission and fusion seem to be essential for mouse development and/or for neuronal survival and function in mice and humans. Mice lacking MFN1, MFN2, or OPA1 die at an early embryonic stage (Chen *et al*, 2003; Davies *et al*, 2007). Moreover, in humans, point mutations in MFN2 and OPA1 lead to severe neurodegenerative diseases such as Charcot–Marie–Tooth type 2A and dominant optic atrophy, respectively (Alexander *et al*, 2000; Delettre *et al*, 2000; Zuchner *et al*, 2004). On the other hand, deletion of DRP1 is lethal for *Caenorhabditis elegans* (Labrousse *et al*, 1999; Breckenridge *et al*, 2008). These findings illustrate the importance of mitochondrial dynamics in cell homeostasis. However, the physiological role of mitochondrial fusion and fission in cell function and survival is still poorly understood. Therefore, the precise mechanism underlying neurodegenerative diseases associated with mitochondrial dynamics defects is unknown.

Fission of mitochondria is required for the selective elimination of depolarized mitochondria (Twig *et al*, 2008), and it occurs during apoptosis (Suen *et al*, 2008). Moreover, mitochondrial fission occurs when mitochondria are dysfunctional, probably as a result of OPA1 cleavage (Duvezin-Caubet *et al*, 2006; Guillery *et al*, 2008). Mitochondrial fission

due to impaired mitochondrial fusion is often accompanied by bioenergetics defects due to a loss of mitochondrial DNA (mtDNA) (Chan, 2006; Hoppins *et al*, 2007). Thus, mitochondrial fusion is required for mtDNA maintenance, probably because it allows mtDNA exchange between mitochondria. Apart from this role, little is known about the importance of mitochondrial fusion. Here we report that mitochondria hyperfuse and form a highly interconnected network in cells exposed to stresses which inhibit cytosolic protein synthesis. Stress-induced mitochondrial hyperfusion (SIMH) requires metabolically active mitochondria, leads to mitochondrial ATP production and confers stress resistance on cells. Therefore, SIMH represents an adaptive response against stress.

Results

MFN1 and OPA1 are required for SIMH

Dramatically elongated mitochondria were found to accumulate in mouse embryonic fibroblasts (MEFs) exposed to a number of stress stimuli, including UV irradiation (UV-C), actinomycin D (Act D), cycloheximide (CHX) (Figure 1A and B), anisomycin, hippuristanol, and serum and amino-acid deprivation (data not shown). It is to be noted that mitochondrial morphological changes were first evidenced at 2–3 h after stress induction and the process increased over time, peaking at 6–9 h with the formation of a mesh of highly interconnected, thin mitochondrial filaments. This morphology could be maintained as long as the cells were exposed to the stress stimuli and did not undergo apoptosis (data not shown). This phenomenon was also observed in a number of mammalian cell lines (HeLa, Cos-7, NIH 3T3, DU145, 143B), in mouse primary fibroblasts, hepatocytes, and astrocytes (data not shown). To reflect the extreme nature of the fusion activity, we named this process 'stress-induced mitochondrial hyperfusion (SIMH).'

To test whether the key molecular components of the mitochondrial fusion machinery are necessary for mitochondrial tubulation during these stresses, we used MEFs deficient in MFN1 (Mfn1$^{-/-}$), MFN2 (Mfn2$^{-/-}$), both MFN1 and 2 (Mfn1/2$^{-/-}$), and OPA1 (Opa1$^{-/-}$) (Chen *et al*, 2003; Song *et al*, 2007). As members of the Bcl-2 family, including BAX

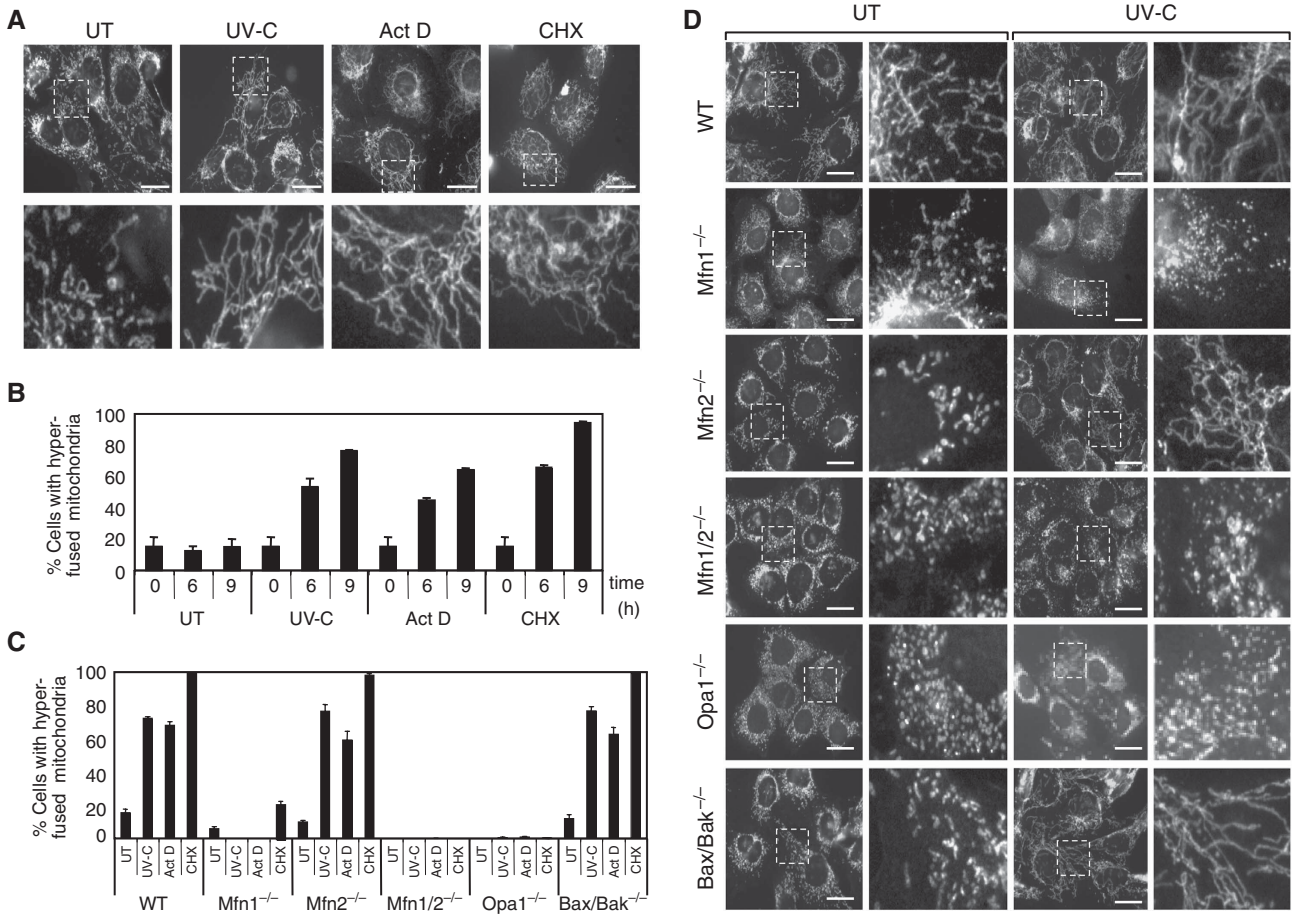

Figure 1 Mitochondrial tubulation in response to stress stimuli requires Opa1 and Mfn1. (**A**, **B**) Wild-type MEFs after exposure to 60 mJ/cm^2 UV-C, 3 μg/ml Act D or 10 μM CHX. (A) MEFs stained with antibodies to cytochrome *c* were analyzed in untreated conditions and 9 h after stress exposure by fluorescence microscopy. Scale bar, 25 μm. (B) Quantification of cells with a majority of connected, very long (>5 μm) tubular mitochondria the extremities of which are difficult to visualize (defined as hyperfused mitochondria) at the indicated time points after stress exposure. Data represent the mean ± s.d. of three independent experiments, each with >300 cells counted per condition. (**C**, **D**) Wild type, Mfn1$^{-/-}$, Mfn2$^{-/-}$, Mfn1/2$^{-/-}$, Opa1$^{-/-}$, and Bax/Bak$^{-/-}$ MEFs after exposure to UV-C irradiation. (C) Quantification of cells with hyperfused mitochondria 9 h after exposure with 60 mJ/cm^2 UV-C, 3 μg/ml Act D, or 10 μM CHX. Data represent the mean ± s.d. of three independent experiments, each with >300 cells counted per condition. Wild-type MEFs shown here are controls for Mfn1$^{-/-}$ cells and are representative of all WT MEFs used as controls for mutant MEFs. (D) MEFs stained with antibodies to cytochrome *c* were analysed in untreated conditions and 9 h after UV-C irradiation by fluorescence microscopy. Scale bar, 25 μm.

and BAK, have recently been reported to modulate mitochondrial morphogenesis (Karbowski *et al*, 2006), we also tested Bax/Bak-deficient MEFs (Bax/Bak$^{-/-}$) (Figure 1C and D). All mutant MEFs displayed small filamentous or punctiform mitochondria, as described earlier (Chen *et al*, 2003; Karbowski *et al*, 2006; Song *et al*, 2007). Exposure of Mfn2$^{-/-}$ and Bax/Bak-deficient cells to Act D, CHX, and UV irradiation induced mitochondrial elongation, which was particularly striking in these cells because small dotty mitochondria 'metamorphosed' into a large number of long, thin filaments (Figure 1C, D and Supplementary movie). Importantly, mitochondrial tubulation did not occur, or was significantly reduced, in cells deficient in OPA1, MFN1, or both mitofusins, indicating a specific role of OPA1 and MFN1, but not MFN2, during SIMH.

Disruption of the mitochondrial membrane potential using the protonophore CCCP or inhibiting the ATP synthase with oligomycin prevented SIMH. Moreover, we found that SIMH did not occur in 143B ρ^0 cells that lack mitochondrial DNA, but display a normal membrane potential (Buchet and Godinot, 1998; Arnould *et al*, 2003) (Supplementary Figure 1A–C). Therefore, an active oxidative phosphorylation is required to promote SIMH.

SIMH results from activation of mitochondrial fusion activity

To determine whether elongation of mitochondria was accompanied by fusion of the inner mitochondrial membrane and continuity of the matrix lumen of fused mitochondria, we first expressed Dendra2, a photoactivable probe, which is photoconverted from green to red on brief excitation with UV, in mitochondria of WT MEFs (Gurskaya *et al*, 2006). The probe was excited in a small region of an elongated mitochondrion and was found to diffuse a long distance from the site of excitation, thereby indicating a continuity of the matrix lumen in the elongated mitochondria of stressed cells (Supplementary Figure 2). Then, we measured mitochondrial fusion activity in stressed Mfn2$^{-/-}$ cells using the mito-PAGFP system, as described earlier (Karbowski *et al*, 2004) (Figure 2A and B). These cells were chosen because of the high reactivity of their mitochondria to stress. At 3 h after CHX addition, mitochondrial fusion activity was significantly increased in Mfn2$^{-/-}$ MEFs when compared to untreated cells. Interestingly, the increase in mitochondrial fusion activity appeared to be a transient event as it decreased after 7 h of CHX treatment.

We also tested the possibility that inhibition of the fission machinery could be part of the mechanism underlying SIMH. Expression of DRP1-K38A, a dominant-negative mutant of Drp1, resulted in mitochondrial elongation in Mfn1$^{-/-}$ as well as in WT and Mfn2$^{-/-}$ cells, but not in Mfn1/2$^{-/-}$ or Opa1$^{-/-}$ cells, confirming the requirement of either Mfn 1 or 2 and OPA1 in the fusion process (Hoppins *et al*, 2007; Figure 2C and D). Opa1$^{-/-}$ cells expressing DRP1-K38A remained SIMH incompetent (data not shown). As inhibiting mitochondrial fission led to tubulation of mitochondria in Mfn1$^{-/-}$ cells, whereas SIMH does not occur in these cells, it is unlikely that DRP1 inhibition is the main mechanism underlying SIMH. Moreover, the protein levels of the fission proteins DRP1 and hFIS1 did not change significantly during the first 9 h after stress exposure (Figure 2E). Finally, overexpression of hFIS1, which fragments mitochondria via DRP1 (Yoon *et al*, 2003), prevented the occurrence of SIMH (data not shown), further indicating that DRP1 activity was not impaired upon stress. Altogether these data suggest that SIMH relies on an increase in mitochondrial fusion activity rather than on an inhibition of the fission activity, even though the latter possibility cannot be completely excluded.

Stomatin-like protein 2 (SLP-2) is required for SIMH

Recently, SLP-2 has been identified as a mitochondrial member of a superfamily of putative scaffolding proteins comprising prohibitins, flotillins, and mechanoreceptors (Tavernarakis *et al*, 1999; Da Cruz *et al*, 2003; Morrow and Parton, 2005; Hajek *et al*, 2007). Even though its function is not yet well characterized, it has recently been found to interact with MFN2 (Hajek *et al*, 2007) and with prohibitins 1 and 2 (Da Cruz *et al*, 2008). We tested whether SLP-2 could also participate in SIMH. We generated MEFs, in which the expression of SLP-2 was downregulated by RNA interference. The morphology and membrane potential of mitochondria were similar in MEFs expressing SLP-2 or luciferase shRNA (Supplementary Figure 3 and data not shown). However, whereas mitochondria from control MEFs underwent SIMH after UV irradiation or CHX treatment, those from SLP-2-depleted MEFs fragmented (Figure 3A and Supplementary Figure 3). Fragmentation of mitochondria occurred within the first 6 h after stress and was not the result of a decrease in mitochondrial membrane potential nor apoptosis (data not shown).

SLP-2 is required for the maintenance of OPA1L during stress

As mitochondria fragmented in SLP-2-deficient stressed cells, we analysed the expression pattern of OPA1, whose modifications have been linked to the regulation of mitochondrial morphology (Duvezin-Caubet *et al*, 2006; Ishihara *et al*, 2006; Griparic *et al*, 2007; Song *et al*, 2007). Five OPA1 bands (a–e) could be detected in control MEFs (Figure 3B). Bands a and b correspond to long isoforms, whereas bands c–e are thought to result from proteolytic processing. In wild-type MEFs, the pattern of OPA1 expression did not change significantly during SIMH. In unstressed SLP-2-deficient MEFs, all OPA1 bands were expressed, but bands c and e were slightly increased in intensity compared to wild-type cells, whereas band d was less intense. On addition of CHX, the intensities of bands a and b decreased significantly, whereas that of bands c and e increased (Figure 3B). Similarly, SLP-2 depletion in Opa1$^{-/-}$ cells transiently transfected with rat OPA1 variant 1 (rOPA1-V1) (Ishihara *et al*, 2006) induced proteolytic cleavage of OPA1 (Figure 4A). Our data thus indicate that, during stress, SLP-2 is required for the maintenance of long OPA1 isoforms.

To examine whether the cleavage of long OPA1 isoforms prevented the occurrence of SIMH in SLP-2-depleted cells, we expressed in these cells a non-cleavable deletion mutant of rat OPA1 variant 1 lacking the S1 cleavage site (rOPA1-V1-ΔS1) (Ishihara *et al*, 2006), as well as a cleavable OPA1 variant 1, rOPA1-V1, as a control. Moderate expression of rOPA1-V1 or rOPA1-V1-ΔS1 did not significantly change the morphology of mitochondria in unstressed SLP-2-depleted cells (Figure 3C). Moreover, during stress only rOPA1-V1-ΔS1, but not rOPA1-V1, promoted SIMH (Figure 3C). Thus, expression of an uncleavable OPA1 long isoform, which

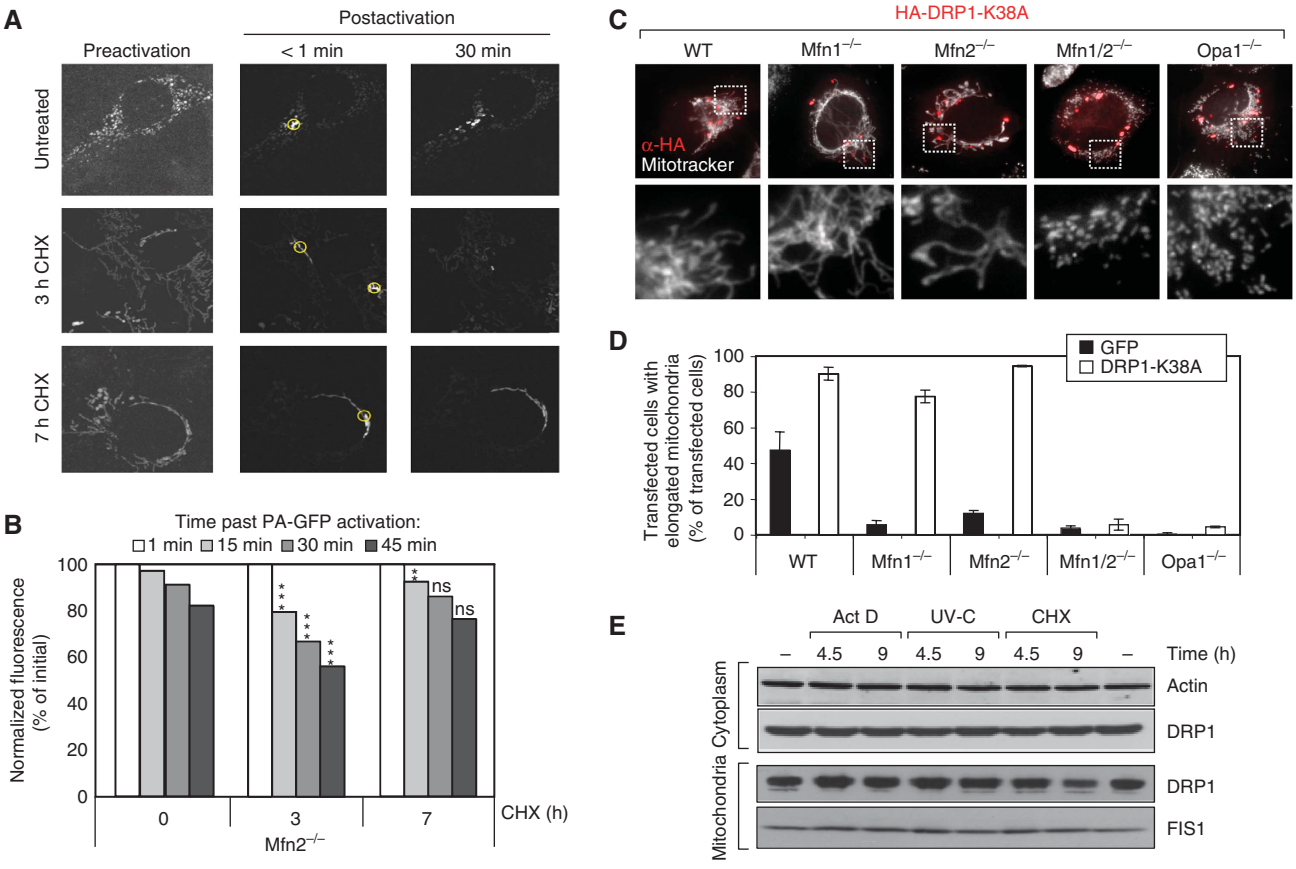

Figure 2 SIMH is a result of increased mitochondrial fusion activity. (**A**) Visualization and (**B**) quantification of mitochondrial fusion using mito-PAGFP in DMSO-treated Mfn2$^{-/-}$ MEFs (UT cells) ($n=27$), as well as Mfn2$^{-/-}$ MEFs 3 h ($n=30$) and 7 h ($n=30$) after CHX treatment. Regions of interest within mito-PAGFP-expressing cells were photoactivated using 405-nm light, followed by whole-cell imaging with 488-nm light. Pre-activation images were taken with higher detector gain, and after the activation the gain was adjusted to avoid oversaturation of activated mitochondria. Post-acquisition processing was performed using MetaMorph software. The data represent mean ± s.e.m. *P*-values (versus untreated Mfn2$^{-/-}$), *t*-test, two-tailed, unpaired. (**C**) Morphology of mitochondria in wild-type, Mfn1$^{-/-}$, Mfn2$^{-/-}$, Mfn1/2$^{-/-}$, and Opa1$^{-/-}$ MEFs transiently expressing the dominant-negative DRP1 mutant HA-DRP1-K38. Mitochondria were stained using MitoTracker and Drp1 K38A revealed using an antibody to HA tag. (**D**) Quantification of cells described in (C) with elongated mitochondrial morphology. As a control, cells were transfected with GFP. Data represent the mean ± s.d. of three independent experiments, each with >300 cells counted per condition. (**E**) Subcellular fractionation of untreated WT MEFs and after exposure to 60 mJ/cm^2 UV-C, 3 μg/ml ActD or 10 μM CHX. Cells were harvested at the indicated time points and mitochondria were isolated. Cytoplasmic and mitochondrial fractions were analysed by SDS–PAGE using antibodies against DRP1 and FIS1, respectively. Actin served as a loading control for the cytoplasmic fraction. The data are representative of three independent experiments. $^{**}P<0.01$; $^{***}P<0.005$; students *t*-test, unpaired, two-tailed.

persisted following CHX treatment (Figure 3D), allowed mitochondria to undergo SIMH in SLP-2-deficient cells. A similar conclusion was drawn from experiments performed with Opa1$^{-/-}$ cells, in which we expressed either rOPA1-V1 or rOPA1-V1-ΔS1 (Figure 4A). Both constructs were able to promote SIMH in control Opa1$^{-/-}$ cells. However, in SLP-2-deficient Opa1$^{-/-}$ cells, only the non-cleavable OPA1 mutant was efficient (Figure 4B). Together, these data allow us to conclude that OPA1 cleavage prevents the occurrence of SIMH in SLP-2-deficient cells. Moreover, these data indicate that the long OPA1 isoform is necessary and sufficient for SIMH (Figure 4C).

To examine whether proteolysis occurred only at the S1 cleavage site, we used rat OPA1 variant 7, which contains both S1 and S2 sites (Ishihara *et al*, 2006). This variant showed the same activity as rOPA1-V1 in stressed normal and SLP-2-deficient Opa1$^{-/-}$ cells (Supplementary Figure 4B). Unstressed SLP-2-deficient cells showed a reduced OPA1 processing at the S2 site and an increased cleavage at the S1 site (Supplementary Figure 4A). Similarly, the S1 cleavage product of isoform 7 (AIF-rOPA1-V7$^{230-997}$) (Ishihara *et al*, 2006) failed to promote fusion in Opa1$^{-/-}$ cells (data not shown).

OPA1 can be cleaved by various proteases (Cipolat *et al*, 2006; Ishihara *et al*, 2006; Duvezin-Caubet *et al*, 2007; Griparic *et al*, 2007; Song *et al*, 2007; Merkwirth *et al*, 2008). To determine whether proteases were responsible for the cleavage of OPA1 in SLP-2-deficient cells during stress, we treated these cells with the serine protease inhibitor PMSF or the metalloprotease inhibitor 1,10-*o*-phenanthroline. As shown in Figure 4D, 1,10-*o*-phenanthroline significantly decreased stress-induced cleavage of OPA1 in SLP-2-deficient MEFs. These data indicate that SLP-2 prevents OPA1 cleavage, probably through metalloproteases, under stress conditions and thereby allows mitochondria to fuse. Altogether, these experiments suggest that SLP-2 controls OPA1 stability during SIMH.

We have recently reported that SLP-2 interacts with prohibitins 1 and 2 (Da Cruz *et al*, 2008), two proteins that are known to control OPA1 processing (Merkwirth *et al*, 2008).

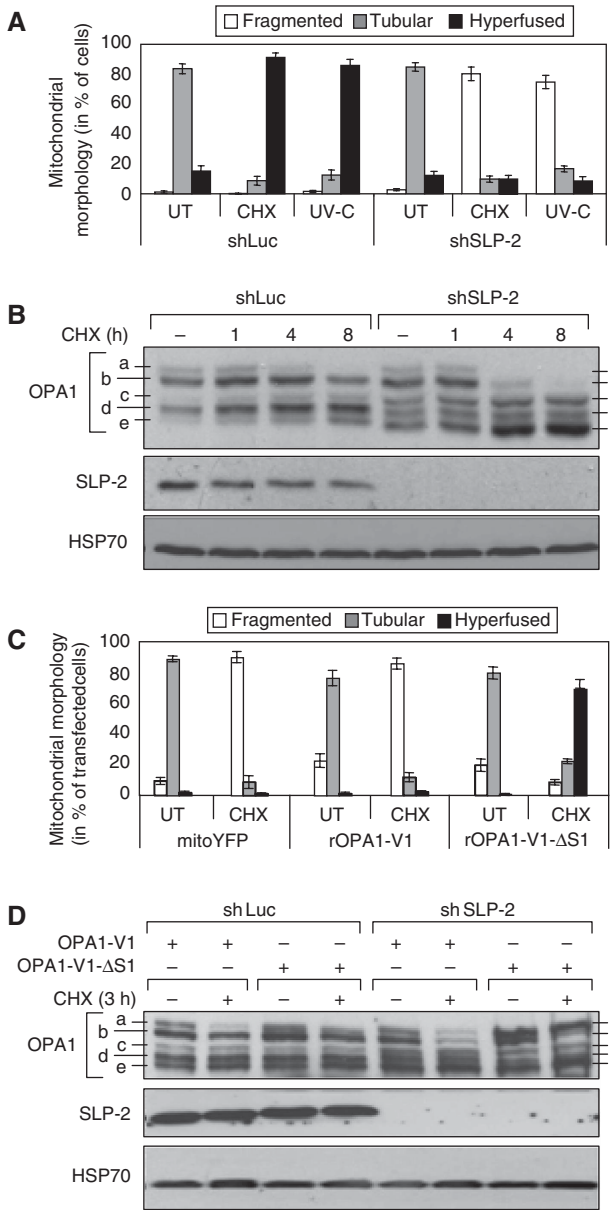

Figure 3 Stress-induced mitochondrial hyperfusion requires SLP-2. (**A**) Quantification of mitochondrial morphology in wild-type MEFs stably expressing control shRNA against Luciferase (shLuc) or shRNA against SLP-2 (shSLP-2) 8 h after exposure to 60 mJ/cm^2 UV-C or 10 μM CHX. Tubular mitochondria are defined as isolated mitochondria with visible free ends; hyperfused mitochondria form a mesh of interconnected organelles, the extremities of which were difficult to visualize. (**B**) Immunoblot analysis of cells described in (A) at the indicated time points after CHX treatment. Whole-cell lysates were analysed by SDS–PAGE using antibodies against OPA1 and SLP-2. (**C**) Quantification of mitochondrial morphology in wild-type MEFs stably expressing shSLP-2 after transient transfection of FLAG-tagged rat OPA1 variant 1 (rOPA1-V1) and its non-cleavable deletion mutant (rOPA1-V1-ΔS1). Cells exposed to 10 μM CHX for 8 h were stained with MitoTracker and antibodies to FLAG, and mitochondrial morphology of transfected cells was analysed by fluorescence microscopy. (**D**) Immunoblot analysis of cells described in (C). Whole-cell lysates were analysed by SDS–PAGE using antibodies against OPA1 and SLP-2. HSP70 served as a loading control (B, D). Data (A, C) represent the mean ± s.d. of three independent experiments, each with >300 cells counted per condition. The blot (B, D) is representative of three independent experiments.

It was therefore possible that the effect of SLP-2 was mediated by prohibitins. To test this hypothesis, we used prohibitin 2 knockout MEFs (Phb2$^{-/-}$), which also lack the expression of prohibitin 1 (Merkwirth *et al*, 2008). On treatment with CHX, we found that mitochondria from Phb2$^{-/-}$ cells fused to the same extent as mitochondria from control cells (Figure 4E and F). Thus, in contrast to the related SLP-2, prohibitins are not required for SIMH.

SIMH promotes optimal mitochondrial ATP production

We next examined the physiological relevance of SIMH. The main role of mitochondria is to produce ATP through oxidative phosphorylation (OXPHOS). We first measured total cellular ATP levels in control and stressed WT MEFs and found a significant increase in ATP in WT MEFs exposed to CHX, UV, or Act D, but not in cells treated with staurosporine (STS), a stimulus that does not trigger SIMH (Figure 5A and data not shown). Similarly, the levels of total ATP increased in CHX-treated Mfn2$^{-/-}$ and shLuc-expressing MEFs. In contrast, no or little increase was measured in CHX-treated Mfn1$^{-/-}$, Opa1$^{-/-}$, and shSLP-2 MEFs (Figure 5B). Thus, total ATP levels increased only in stressed SIMH-competent cells. Although relative ATP amounts are shown, absolute values of ATP were comparable in unstressed WT, Mfn1$^{-/-}$, and Mfn2 $^{-/-}$ MEFs, despite a small increase of ATP in Mfn1$^{-/-}$ MEFs (Supplementary Figure 5). To test whether mitochondria were responsible for the increase in ATP production, we tested their OXPHOS capacity. We provided methylpyruvate, an oxidative respiratory substrate, to adherent cells and measured the production of ATP over 15 min. Such a question cannot be addressed with purified mitochondria, which inevitably fragment during mitochondrial isolation. Figure 5C shows that in unstressed WT cells, methylpyruvate caused a minor increase in ATP levels over the 15-min period. In contrast, when added to WT cells that had been pretreated with CHX for 6 h, methylpyruvate stimulated ATP production. This increase was abolished by the ATP synthase inhibitor oligomycin, confirming its mitochondrial origin (Figure 5C). Setting the ATP levels in all unstressed cells at 100%, we also measured a 20–40% increase in ATP levels over a 15-min time course in stressed Mfn2$^{-/-}$ cells (Figure 5D). In contrast, in CHX-treated Mfn1$^{-/-}$ cells (Figure 5D) and SLP-2-deficient cells (Figure 5E), the levels of ATP remained stable after addition of methylpyruvate. Reintroduction of SLP-2 in the SLP-2-deficient MEFs rendered these cells SIMH competent and allowed an increased OXPHOS after stress (Figure 5E). Thus, the increase in total ATP levels measured in cells undergoing SIMH is due, at least in part, to increased OXPHOS. Part of these ATP levels could also be because of decreased ATP hydrolysis.

An ultrastructural analysis of mitochondria from WT MEFs undergoing SIMH revealed organelles with a condensed matrix and swollen cristae, a structure consistent with an increased oxidative phosphorylation (Hackenbrock, 1966) (Figure 6). Surprisingly, mitochondria in stressed Mfn1$^{-/-}$ and Opa1$^{-/-}$ MEFs also adopted the 'condensed state' morphology with enlarged cristae (Figure 6), despite no apparent increase in OXPHOS (Figure 5D). These findings suggest that mitochondrial hyperfusion is required for optimal OXPHOS. In contrast, in SLP-2-deficient cells, whereas the mitochondria displayed an orthodox morphology in the absence of stress, cristae remodelled during stress and formed

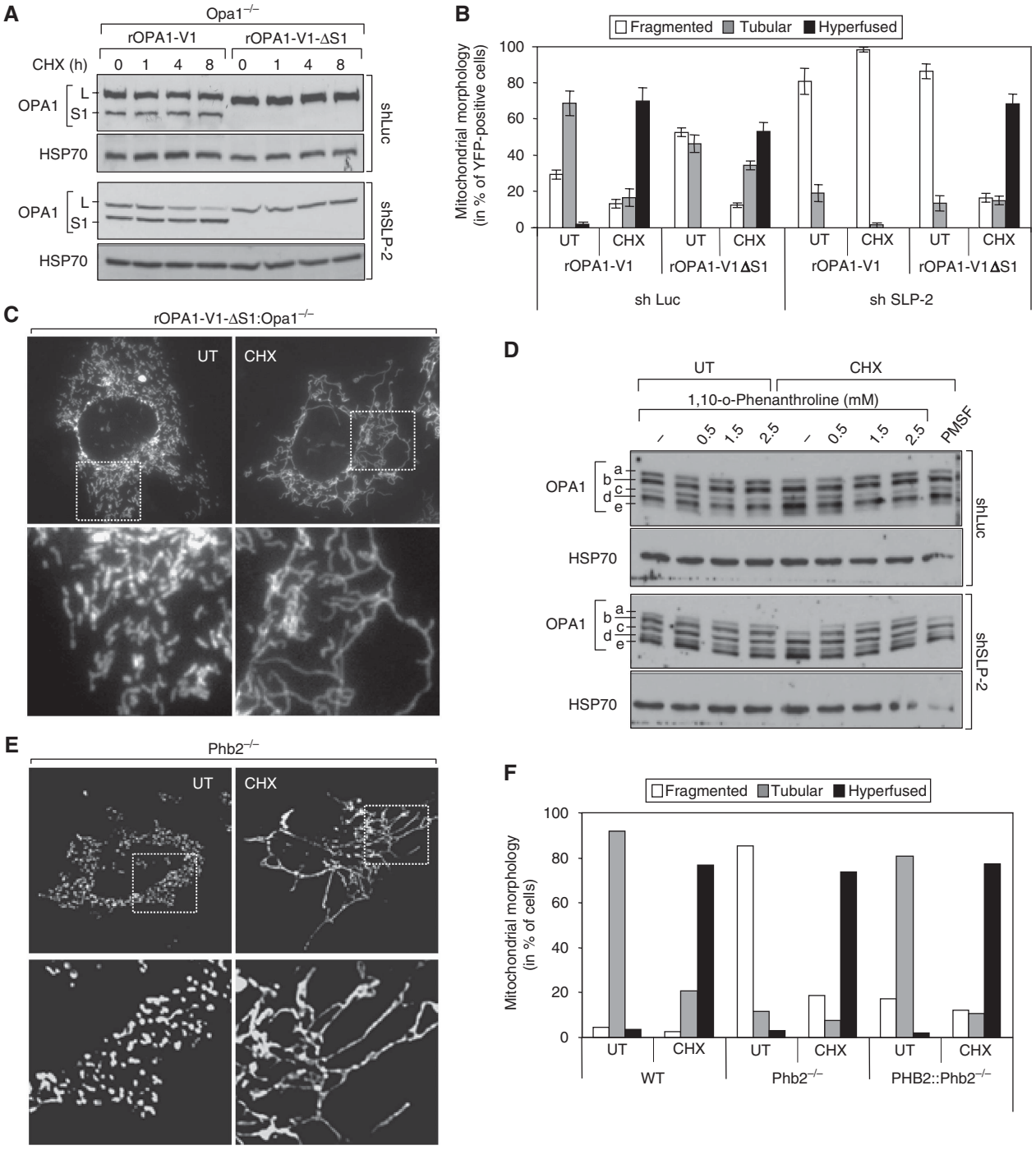

Figure 4 SLP-2 prevents OPA1 proteolysis during SIMH. (**A**) Immunoblot analysis of Opa1$^{-/-}$ MEFs stably expressing shSLP-2 or shLuc after transient transfection of FLAG-tagged rat OPA1 variant 1 (rOPA1-V1) and its non-cleavable deletion mutant (rOPA1-V1-ΔS1) at the indicated time points after CHX treatment. Whole-cell lysates were analysed by SDS–PAGE using antibodies against OPA1. (**B**) Quantification of mitochondrial morphology in Opa1$^{-/-}$ MEFs stably expressing shLuc or shSLP-2 after transient transfection of mitochondrial targeted YFP alone (not shown) or together with rOPA1-V1 and rOPA1-V1-ΔS1. Cells were exposed to 10 μM CHX for 8 h and YFP-positive cells were analysed by fluorescence microscopy (**C**). (**D**) Wild-type MEFs stably expressing shRNA against Luciferase (shLuc) or SLP-2 (shSLP-2) were treated with indicated concentrations of (1,10)-*o*-phenanthroline or 1 mM PMSF alone or in combination with 10 μM CHX. After 3 h, cells were harvested and whole-cell lysates were used for SDS–PAGE. (**E**) Mitochondrial morphology in Pbh2$^{fl/fl}$ MEFs (WT), Prohibitin 2 knockout (Phb2$^{-/-}$) and Phb2$^{-/-}$ re-expressing prohibitin 2 (PHB2::Phb2$^{-/-}$) 6 h after exposure to 10 μM CHX. (**F**) Quantification of cells shown in (E). HSP70 served as a loading control (A, D). Data (B) represent the mean ± s.d. of three independent experiments, each with >300 cells counted per condition.

large, disorganized vesicles (Figure 6). Altogether, these data indicate that SIMH provides cells with increased OXPHOS and ATP levels, and suggested that this process could help cells overcome transient, reversible metabolic insults.

SIMH is a pro-survival response against stress

We studied whether SIMH could act as a protective response against UV irradiation or Act D treatment, two stimuli that induce SIMH. These studies were performed with Mfn1$^{-/-}$,

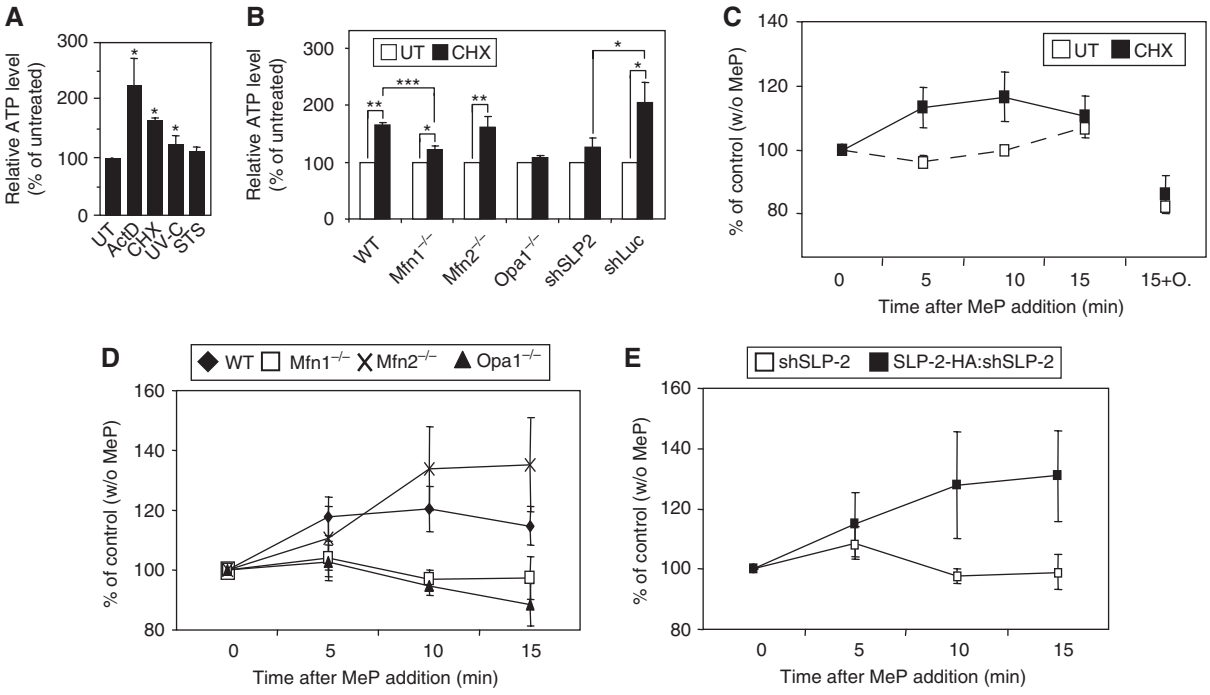

Figure 5 SIMH promotes mitochondrial ATP production. (**A**, **B**) Measurement of total ATP levels in WT MEFs treated with Act D (3 μM), CHX (10 μM), UV (60 mJ/cm^2), and STS (0.25 μM) (A), in SIMH competent (WT, Mfn2$^{-/-}$, shLuc) and incompetent (Mfn1$^{-/-}$, OPA1$^{-/-}$, shSLP-2) cells (B) exposed to 10 μM CHX treatment for 6 h. (**C**–**E**) Measurement of mitochondrial ATP production. Cells were pretreated with 10 μM CHX for 6 h, followed by 10 mM methylpyruvate (MeP). Cells were harvested after 5, 10 or 15 min and total ATP levels assayed. In (C) ATP levels were also measured 15 min after co-addition of methylpyruvate + oligomycin (10 μM). Data represent the mean ± s.e.m of at least three independent experiments. *$P<0.05$; **$P<0.01$; ***$P<0.005$; students *t*-test, unpaired, two-tailed.

SLP-2-deficient cells, and control cells. Apoptosis was evidenced only at late time points (>14 h). Figures 7A and B show that the SIMH-incompetent cells, Mfn1$^{-/-}$, and SLP-2-deficient MEFs or HeLa cells displayed a high sensitivity to Act D and UV irradiation as compared with SIMH-competent cells (hMFN1-HA:Mfn1$^{-/-}$ and shLuc cells). Importantly, Mfn1$^{-/-}$ and hMfn1-HA:Mfn1$^{-/-}$ cells were equally sensitive to staurosporine, a stimulus that does not trigger SIMH (Figure 7C and data not shown). This indicates that the SIMH-incompetent cells are not vulnerable to all apoptotic stimuli, but that their sensitivity is cell context specific. The resistance of SIMH-competent cells was explained by a delay in BAX activation and cytochrome *c* release, both assessed by immunocytochemistry (Supplementary Figure 6). In addition, when cells were stressed during 4 h with a low dose of Act D that was sufficient to induce SIMH, they acquired a long-lasting resistance to a secondary apoptotic stress (Supplementary Figure 7). Thus, these data show that SIMH represents a pro-survival response against specific stress stimuli and indicate that this process could act as a pre-conditioning mechanism against specific apoptotic stresses.

Discussion

One of the central questions of mitochondrial dynamics is what physiological role this process plays in cell homeostasis. We show that during various stress responses leading to protein synthesis inhibition, mitochondria hyperfuse, a process we called stress-induced mitochondrial hyperfusion (SIMH). SIMH was found to correlate with increased mitochondrial ATP production and to confer on cells a resistance to stress.

Mitochondria can rapidly change their morphology in response to many stress conditions. Stimuli that alter mitochondrial function often result in fission of the organelle (Baricault *et al*, 2007; Duvezin-Caubet *et al*, 2007; Guillery *et al*, 2008). Rarely has mitochondrial fusion been described as a response to stress as reported here. Several decades ago, Deitch and Godman (1967) reported that low Act D concentration triggers mitochondrial 'anastomosing networks' in HeLa cells. Moreover, abnormally elongated mitochondria have been described in cells of tobacco in response to hypoxia (Van Gestel and Verbelen, 2002), and in mammalian cells exposed to the alkylating chemical ethacrinic acid, even though in this case the chemical may have exerted its action by non-specifically inhibiting fission proteins (Soltys and Gupta, 1994; Bowes and Gupta, 2008). Mitochondrial elongation has also been reported in cultured cells enforced to produce ATP through OXPHOS for several days (Rossignol *et al*, 2004). In our study, we report that several stimuli, including mRNA translation inhibitors, UV irradiation, and Act D, which share the property of downregulating protein synthesis (Siegel and Sisler, 1963; Grollman, 1967; Craig and Kostura, 1983; Parker *et al*, 2006), can trigger mitochondrial fusion (SIMH). Our genetic data suggest a prominent role of OPA1 and MFN1 during SIMH. OPA1 is responsible for inner mitochondrial membrane fusion and cristae organization (Sesaki *et al*, 2003; Wong *et al*, 2003; Cipolat *et al*, 2006; Frezza *et al*, 2006). Various OPA1 short and long isoforms are present in mammals as a result of alternative splicing and proteolysis. Short and long isoforms have been shown to be

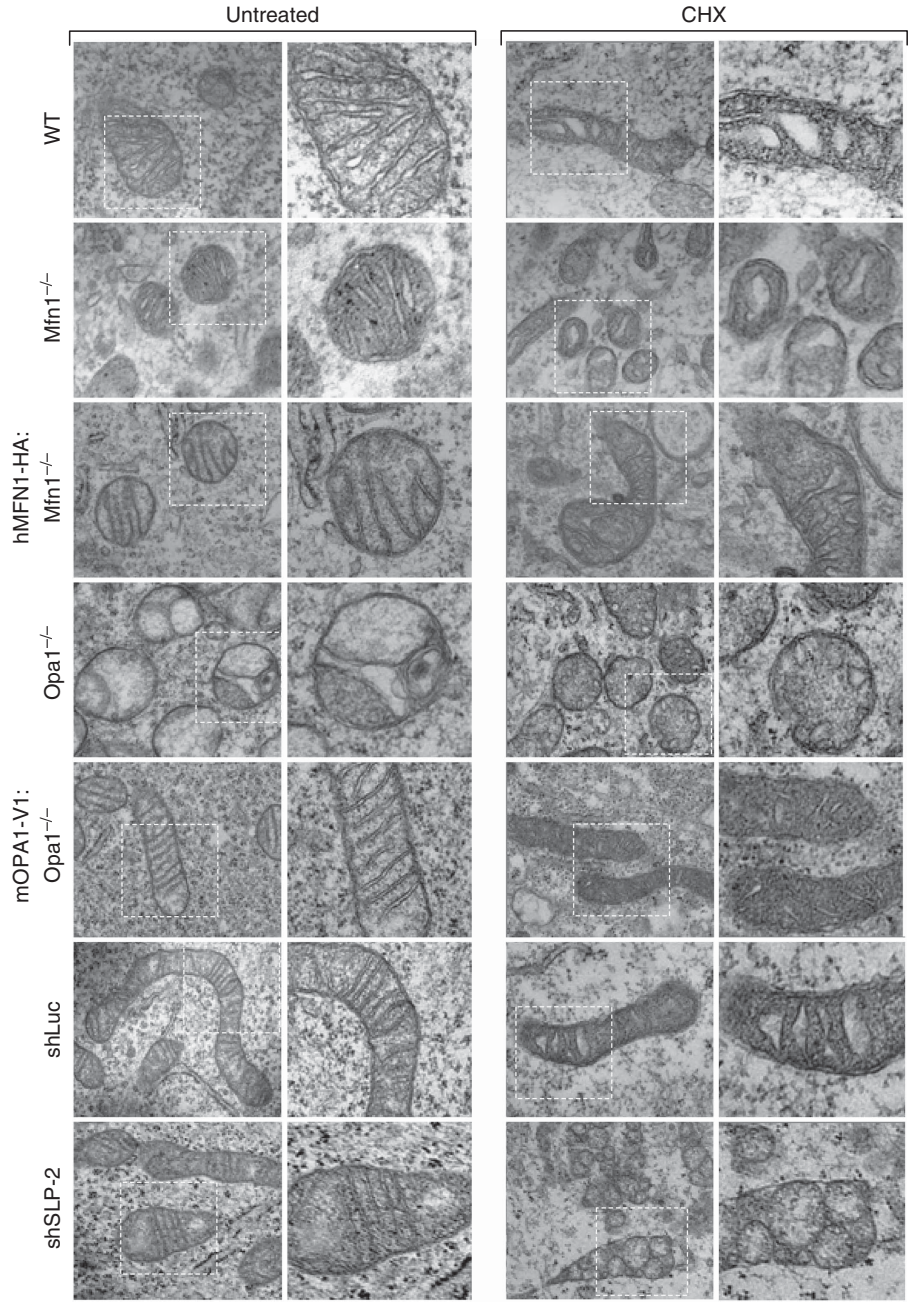

Figure 6 SIMH is associated with ultrastructural changes. Ultrastructural analysis of WT, $Mfn1^{-/-}$, hMFN1-HA:$Mfn1^{-/-}$, $OPA1^{-/-}$, mOPA1-V1:$OPA1^{-/-}$, shLuc, and shSLP-2 MEFs. Cells were untreated (left part) or exposed to 10 μM CHX (right part) and fixed after 6 h for electron microscopy analysis. Scale bar, 1 μm.

required for optimal mitochondrial fusion under normal conditions (Song *et al*, 2007), although Ishihara *et al* (2006) have reported that mitochondrial fusion could occur with only the L-OPA1 isoform. The long OPA1 isoform is necessary and sufficient to promote SIMH. This finding is supported by the observation that mitochondria fuse in Yme1L1-deficient cells that lack S-OPA1 (Griparic *et al*, 2007).

The maintenance of L-OPA1 during stress is ensured by SLP-2, a mitochondrial inner-membrane protein, recently identified as a member of the SPFH-family (prohibitin/stomatin/flotillin/Hflk) of putative scaffolding proteins. We have earlier shown a physical interaction between SLP-2 and prohibitins 1 and 2 (Da Cruz *et al*, 2008), which control OPA1 processing (Merkwirth *et al*, 2008). However, knockout of prohibitins did not prevent SIMH, indicating that SLP-2 regulates OPA1 processing under stress conditions independently of prohibitins. Our findings thus indicate that different mechanisms control mitochondrial fusion under normal growth conditions and under stress. MFN2, BAX, and BAK, as well as prohibitins, are required to maintain a tubular mitochondrial network and fusion under normal growth conditions, but are not necessary for SIMH. SLP-2, on the other hand, is required for mitochondrial fusion under stress conditions.

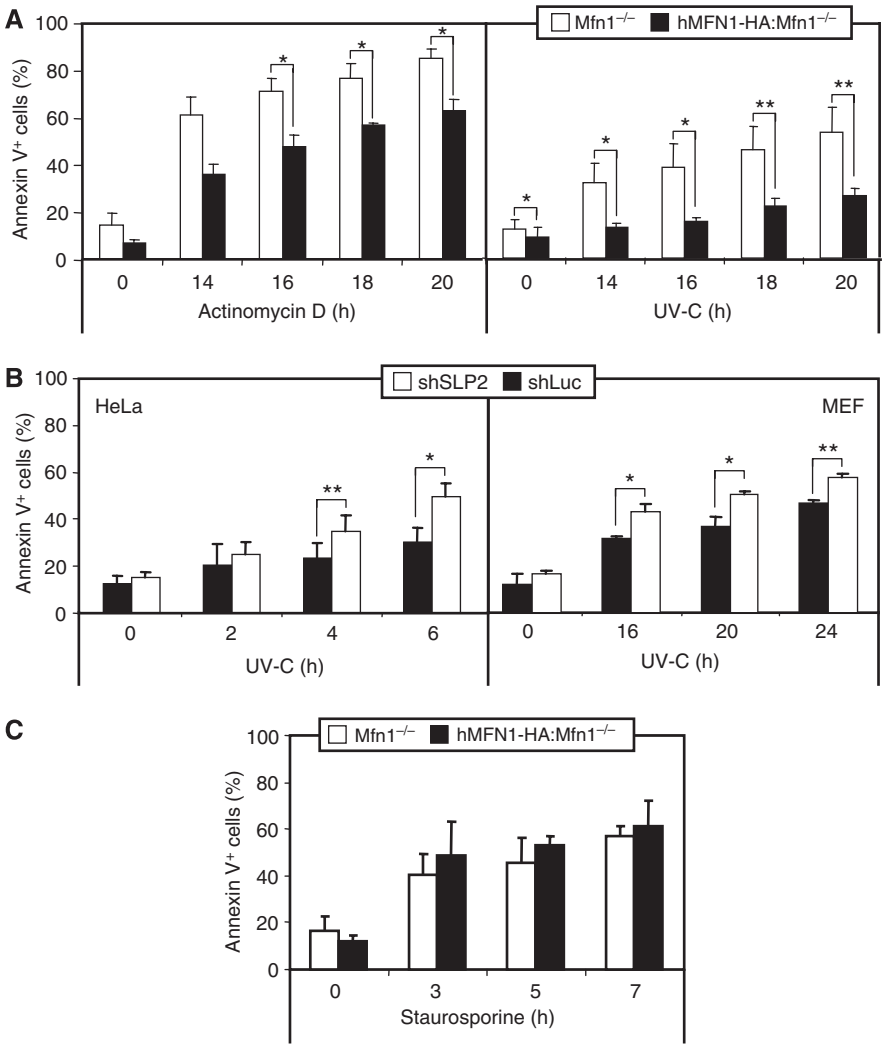

Figure 7 Stress-induced mitochondrial hyperfusion protects against apoptosis. (**A**) Death of $Mfn1^{-/-}$ and hMFN1-HA:$Mfn1^{-/-}$ cells exposed to 3 μg/ml Act D or 60 mJ/cm^2 UV-C. (**B**) Death of HeLa and MEF cells transiently transfected with shSLP-2 or shLuc after exposure to 60 mJ/cm^2 UV-C. (**C**) Death of $Mfn1^{-/-}$ and hMFN1-HA:$Mfn1^{-/-}$ MEF cells exposed to 1 μM staurosporine. In all cases cells were harvested at the indicated time points and stained with annexin V FITC for flow-cytometric analysis. Data represent the mean ± s.e.m of at least three independent experiments (*$P<0.05$; **$P<0.01$).

We found that SIMH competent cells show better resistance to SIMH-inducing stresses, UV irradiation, and Act D treatment, when compared with SIMH-incompetent cells. Mitochondrial hyperfusion correlates with a delay in BAX activation and MOMP, a result that is consistent with the earlier-reported beneficial effect of mitofusin overexpression (Sugioka *et al*, 2004), although in this study the resistance conferred by enforced mitochondrial fusion was not restricted to stimuli that induce SIMH. Our results point to an important role of SIMH for the maintenance of mitochondrial ATP production under stress. We found that during SIMH mitochondria adopt the so-called condensed morphology, first described by Hackenbrock (1966), and produce increased levels of ATP, despite a decrease in mitochondrial respiration (not shown). Interestingly, in the SIMH incompetent cells, $Mfn1^{-/-}$, and $Opa1^{-/-}$ cells, despite condensation of their matrix, mitochondria did not produce higher ATP levels on stress. These findings suggest that fusion of the organelle is necessary to provide optimal mitochondrial functioning. It has been theorized earlier that mitochondrial fusion would generate networks of elongated mitochondria with continuous membranes and matrix lumen, allowing a free diffusion of molecules such as ADP, NADH, $FADH_2$, and resulting in optimal OXPHOS (Skulachev, 2001). However, so far all approaches whereby mitochondria were enforced to fuse, through for example downregulation of fission proteins, led to opposite results, that is, decrease in membrane potential and ATP production, probably because unbalancing fission and fusion processes damage mitochondria (Rossignol *et al*, 2004; Parone *et al*, 2008; Twig *et al*, 2008). To our knowledge, our findings are the first to show that physiological elongation and fusion of mitochondria correlate with improved mitochondrial function.

Materials and methods

Reagents and antibodies

Please refer to the Supplementary data for detailed description.

Cell lines

$Mfn1^{-/-}$, $Mfn2^{-/-}$, $Mfn1/2^{-/-}$, and $Opa1^{-/-}$ were generated as described (Chen *et al*, 2005; Song *et al*, 2007). $Bax/Bak^{-/-}$ and $143B\rho^0$ cells were kindly provided by Professor S Korsmeyer and

Professor R Wiesner, respectively. Cells were cultivated in high-glucose Dulbecco's modified Eagle's medium supplemented with 10% fetal bovine serum, 100 U/ml penicillin, 0.1 mg/ml streptomycin, and 2 mM glutamine and maintained in 5% CO_2 at 37°C. For transient transfections cells were plated in culture dishes 45 min before transfection and transfected using a calcium phosphate coprecipitation method.

Generation of stable cell lines

MEFs stably expressing shRNAs were generated as described (Parone *et al*, 2006; Da Cruz *et al*, 2008). This method is described in the Supplementary data.

Immunocytochemistry and quantification of mitochondrial morphology

To visualize the mitochondrial network with MitoTracker Red staining, cells grown on coverslips were incubated in growth medium supplemented with 100 nM MitoTracker Red for 10 min, washed in fresh warm medium, and fixed as described above. The coverslips were incubated in cold acetone for 10 min at −20°C, then washed with PBS, mounted, and visualized as described below. For mitochondrial morphology quantifications, mitochondria were stained for immunofluorescence using MitoTracker or anti-cytochrome *c* antibodies, as described earlier (Parone *et al*, 2006). Cells displaying a highly interconnected, tubular mitochondrial network were counted. Mitochondrial morphology was analysed using an Axiophot or LSM510 meta confocal microscope (Zeiss, Germany).

Quantification of mitochondrial fusion activity using the mitochondrially targeted photoactivatible GFP (mtPA-GFP) has been described earlier (Karbowski *et al*, 2004).

Fluorescence time-lapse microscopy

$Mfn2^{-/-}$ MEFs were transfected with the pDsRed-mito (Clontech, Invitrogen) coding plasmid as described above. At 24 h after transfection, cells were plated in 35-mm glass bottom dishes (WillCo-dish, type 3522, WillCo Wells BV). At 2 h before observation, the media was changed to imaging media (DMEM 10% FCS without phenol red). Sixty minutes before recording, cells were UV-irradiated. The cultures were placed in a 37°C chamber equilibrated with humidified air containing 5% CO_2 throughout videomicroscopy. Time-lapse microscopy was performed with a Leica Microsystems AS MDW microscope using a ×63 glycerol objective (NA 1.3). The cells were illuminated every 20 min for 52 ms (excitation at 545 nm), and time-lapse series of 30 z-stacks with 0.2 μm step size were captured with a TRITC filter set during 15 h. The movies were created from the time-lapse series using Leica AS MDW, AutoDeblur (AutoQuant), and Image J softwares. Briefly, the individual z-slices were submitted to deconvolution with AutoDeblur (AutoQuant) software, and a maximum-intensity projection on a single plane of the processed images was created using the Image J software.

Immunoblotting

Cells were resuspended in lysis buffer: 10 mM HEPES, 300 mM KCl, 5 mM $MgCl_2$, 1 mM EGTA, 1% Triton X-100 (vol/vol), 0.1% (wt/vol) sodium dodecyl sulphate (SDS), pH 7.4, supplemented with 1× proteinase inhibitor mixture (Roche). The lysate was spun at 2000 *g*, and the protein concentration was determined by a Bradford assay (Bio-Rad). Equal amounts of protein were subjected to SDS–polyacrylamide gel electrophoresis, transferred to nitrocellulose membranes (Schleicher & Schuell), immunoblotted with primary antibodies followed by horseradish peroxidase-conjugated secondary antibodies, and developed by enhanced chemiluminescence.

Measurement of ATP levels

ATP levels were measured using the ATP Determination Kit (Invitrogen) according to the manufacturer's protocol.

Electron microscopy

Cells were fixed for 20 min at RT in culture medium supplemented with 2.5% glutaraldehyde. After a wash in 100 mM phosphate buffer (KH_2/Na_2HPO_4; pH 7.4), cells were post-fixed for 20 min at RT in 2% osmium tetroxide (OSO_4), and pre-stained in 2% of uranyl acetate for 10 min at RT. After washes in phosphate buffer, cells were dehydrated in 50, 70, 90, and 100% ethanol (for 10 min for each procedure). The samples were then infiltrated sequentially in 1:1 (vol/vol) ethanol:Spurr resin (Polyscience), 1:3 ethanol:Spurr resin for 30 min for each procedure, 100% Spurr resin for 3 h, and finally 100% Spurr resin for 48 h at 60°C for polymerization.

Ultrathin sections were isolated on nickel grids and stained for 10 min in 2% uranyl acetate and for 5 min in Reynold's lead citrate, and examined at 60 kV using a Philips M400 transmission electron microscope.

Apoptosis

Apoptosis was detected using Annexin V FITC (BD Bioscience) as described earlier (Parone *et al*, 2006). Apoptosis in cells expressing shLuc or shSLP-2 was performed as follows: MEFs or HeLa cells were transiently transfected with either pRETROshLuc or pRETROshSLP-2 plasmid, together with a plasmid encoding a red fluorescent protein (ptdTomato-C1) used as a marker of cell transfection. At 72 h post-transfection, cells were exposed to UV-C, collected at different time points as indicated, and stained with Annexin V-FITC. Apoptosis of Tomato-red-labelled cells was performed by flow cytometry.

Supplementary data

Supplementary data are available at *The EMBO Journal* Online (http://www.embojournal.org).

Acknowledgements

We thank Dr Mihara and Dr Ishihara for rat OPA1-V1, OPA1-V1ΔS1, OPA1-V7, and AIF-OPA1-$V7^{230–997}$ cDNAs, Dr Scorrano for OPA1 cDNA, Dr Rojo for human Mfn1 cDNA, Professor Wiesner for 143B rho0 cells, Professor Picard for pdtTomato-C1, Dr Dencher and Dr Madrenas for support, Dr Rossignol for his advices and all members of the lab for fruitful discussions. This work was funded by the Deutsche Forschungsgemeinschaft (DFG) (TO540/1-1), the NIH intramural program, the Swiss National Science Foundation (subsidy 3100A0-109419/1), Oncosuisse Trust, Roche Reasearch Foundation and the Geneva Department of Education. FK is funded in part by the European Union (MiMage, EC FP6 Contract No. LSHM-CT-2004-512020).

References

Alexander C, Votruba M, Pesch UE, Thiselton DL, Mayer S, Moore A, Rodriguez M, Kellner U, Leo-Kottler B, Auburger G, Bhattacharya SS, Wissinger B (2000) OPA1, encoding a dynamin-related GTPase, is mutated in autosomal dominant optic atrophy linked to chromosome 3q28. *Nat Genet* **26:** 211–215

Arnould T, Mercy L, Houbion A, Vankoningsloo S, Renard P, Pascal T, Ninane N, Demazy C, Raes M (2003) mtCLIC is up-regulated and maintains a mitochondrial membrane potential in mtDNA-depleted L929 cells. *Faseb J* **17:** 2145–2147

Baricault L, Segui B, Guegand L, Olichon A, Valette A, Larminat F, Lenaers G (2007) OPA1 cleavage depends on decreased mitochondrial ATP level and bivalent metals. *Exp Cell Res* **313:** 3800–3808

Bowes T, Gupta RS (2008) Novel mitochondrial extensions provide evidence for a link between microtubule-directed movement and mitochondrial fission. *Biochem Biophys Res Commun* **376:** 40–45

Breckenridge DG, Kang BH, Kokel D, Mitani S, Staehelin LA, Xue D (2008) Caenorhabditis elegans drp-1 and fis-2 regulate distinct cell-death execution pathways downstream of ced-3 and independent of ced-9. *Mol Cell* **31:** 586–597

Buchet K, Godinot C (1998) Functional F1-ATPase essential in maintaining growth and membrane potential of human mitochondrial DNA-depleted rho degrees cells. *J Biol Chem* **273:** 22983–22989

Chan DC (2006) Mitochondria: dynamic organelles in disease, aging, and development. *Cell* **125:** 1241–1252

Chen H, Chomyn A, Chan DC (2005) Disruption of fusion results in mitochondrial heterogeneity and dysfunction. *J Biol Chem* **280:** 26185–26192

Chen H, Detmer SA, Ewald AJ, Griffin EE, Fraser SE, Chan DC (2003) Mitofusins Mfn1 and Mfn2 coordinately regulate mitochondrial fusion and are essential for embryonic development. *J Cell Biol* **160:** 189–200

Cipolat S, Martins de Brito O, Dal Zilio B, Scorrano L (2004) OPA1 requires mitofusin 1 to promote mitochondrial fusion. *Proc Natl Acad Sci USA* **101:** 15927–15932

Cipolat S, Rudka T, Hartmann D, Costa V, Serneels L, Craessaerts K, Metzger K, Frezza C, Annaert W, D'Adamio L, Derks C, Dejaegere T, Pellegrini L, D'Hooge R, Scorrano L, De Strooper B (2006) Mitochondrial rhomboid PARL regulates cytochrome *c* release during apoptosis via OPA1-dependent cristae remodeling. *Cell* **126:** 163–175

Craig N, Kostura M (1983) Inhibition of protein synthesis in CHO cells by actinomycin D: lesion occurs after 40S initiation complex formation. *Biochemistry* **22:** 6064–6071

Da Cruz S, Parone PA, Gonzalo P, Bienvenut WV, Tondera D, Jourdain A, Quadroni M, Martinou JC (2008) SLP-2 interacts with prohibitins in the mitochondrial inner membrane and contributes to their stability. *Biochim Biophys Acta* **1783:** 904–911

Da Cruz S, Xenarios I, Langridge J, Vilbois F, Parone PA, Martinou JC (2003) Proteomic analysis of the mouse liver mitochondrial inner membrane. *J Biol Chem* **278:** 41566–41571

Davies VJ, Hollins AJ, Piechota MJ, Yip W, Davies JR, White KE, Nicols PP, Boulton ME, Votruba M (2007) Opa1 deficiency in a mouse model of autosomal dominant optic atrophy impairs mitochondrial morphology, optic nerve structure and visual function. *Hum Mol Genet* **16:** 1307–1318

Deitch AD, Godman GC (1967) Cytology of cultured cells surviving actinomycin D. *Proc Natl Acad Sci USA* **57:** 1607–1610

Delettre C, Lenaers G, Griffoin JM, Gigarel N, Lorenzo C, Belenguer P, Pelloquin L, Grosgeorge J, Turc-Carel C, Perret E, Astarie-Dequeker C, Lasquellec L, Arnaud B, Ducommun B, Kaplan J, Hamel CP (2000) Nuclear gene OPA1, encoding a mitochondrial dynamin-related protein, is mutated in dominant optic atrophy. *Nat Genet* **26:** 207–210

Duvezin-Caubet S, Jagasia R, Wagener J, Hofmann S, Trifunovic A, Hansson A, Chomyn A, Bauer MF, Attardi G, Larsson NG, Neupert W, Reichert AS (2006) Proteolytic processing of OPA1 links mitochondrial dysfunction to alterations in mitochondrial morphology. *J Biol Chem* **281:** 37972–37979

Duvezin-Caubet S, Koppen M, Wagener J, Zick M, Israel L, Bernacchia A, Jagasia R, Rugarli EI, Imhof A, Neupert W, Langer T, Reichert AS (2007) OPA1 processing reconstituted in yeast depends on the subunit composition of the m-AAA protease in mitochondria. *Mol Biol Cell* **18:** 3582–3590

Frezza C, Cipolat S, Martins de Brito O, Micaroni M, Beznoussenko GV, Rudka T, Bartoli D, Polishuck RS, Danial NN, De Strooper B, Scorrano L (2006) OPA1 controls apoptotic cristae remodeling independently from mitochondrial fusion. *Cell* **126:** 177–189

Griparic L, Kanazawa T, van der Bliek AM (2007) Regulation of the mitochondrial dynamin-like protein Opa1 by proteolytic cleavage. *J Cell Biol* **178:** 757–764

Grollman AP (1967) Inhibitors of protein biosynthesis. II. Mode of action of anisomycin. *J Biol Chem* **242:** 3226–3233

Guillery O, Malka F, Frachon P, Milea D, Rojo M, Lombes A (2008) Modulation of mitochondrial morphology by bioenergetics defects in primary human fibroblasts. *Neuromuscul Disord* **18:** 319–330

Gurskaya NG, Verkhusha VV, Shcheglov AS, Staroverov DB, Chepurnykh TV, Fradkov AF, Lukyanov S, Lukyanov KA (2006) Engineering of a monomeric green-to-red photoactivatable fluorescent protein induced by blue light. *Nat Biotechnol* **24:** 461–465

Hackenbrock CR (1966) Ultrastructural bases for metabolically linked mechanical activity in mitochondria. I. Reversible ultrastructural changes with change in metabolic steady state in isolated liver mitochondria. *J Cell Biol* **30:** 269–297

Hajek P, Chomyn A, Attardi G (2007) Identification of a novel mitochondrial complex containing mitofusin 2 and stomatin-like protein 2. *J Biol Chem* **282:** 5670–5681

Hoppins S, Lackner L, Nunnari J (2007) The machines that divide and fuse mitochondria. *Annu Rev Biochem* **76:** 751–780

Ishihara N, Fujita Y, Oka T, Mihara K (2006) Regulation of mitochondrial morphology through proteolytic cleavage of OPA1. *EMBO J* **25:** 2966–2977

Karbowski M, Arnoult D, Chen H, Chan DC, Smith CL, Youle RJ (2004) Quantitation of mitochondrial dynamics by photolabeling of individual organelles shows that mitochondrial fusion is blocked during the Bax activation phase of apoptosis. *J Cell Biol* **164:** 493–499

Karbowski M, Norris KL, Cleland MM, Jeong SY, Youle RJ (2006) Role of Bax and Bak in mitochondrial morphogenesis. *Nature* **443:** 658–662

Koshiba T, Detmer SA, Kaiser JT, Chen H, McCaffery JM, Chan DC (2004) Structural basis of mitochondrial tethering by mitofusin complexes. *Science* **305:** 858–862

Labrousse AM, Zappaterra MD, Rube DA, van der Bliek AM (1999) C. elegans dynamin-related protein DRP-1 controls severing of the mitochondrial outer membrane. *Mol Cell* **4:** 815–826

Merkwirth C, Dargazanli S, Tatsuta T, Geimer S, Lower B, Wunderlich FT, von Kleist-Retzow JC, Waisman A, Westermann B, Langer T (2008) Prohibitins control cell proliferation and apoptosis by regulating OPA1-dependent cristae morphogenesis in mitochondria. *Genes Dev* **22:** 476–488

Morrow IC, Parton RG (2005) Flotillins and the PHB domain protein family: rafts, worms and anaesthetics. *Traffic* **6:** 725–740

Parker SH, Parker TA, George KS, Wu S (2006) The roles of translation initiation regulation in ultraviolet light-induced apoptosis. *Mol Cell Biochem* **293:** 173–181

Parone PA, Da Cruz S, Tondera D, Mattenberger Y, James D, Maechler P, Barja F, Martinou JC (2008) Preventing mitochondrial fission impairs mitochondrial function and leads to loss of mitochondrial DNA. *PLoSONE* **3:** e3257

Parone PA, James DI, Da Cruz S, Mattenberger Y, Donze O, Barja F, Martinou JC (2006) Inhibiting the mitochondrial fission machinery does not prevent Bax/Bak-dependent apoptosis. *Mol Cell Biol* **26:** 7397–7408

Rossignol R, Gilkerson R, Aggeler R, Yamagata K, Remington SJ, Capaldi RA (2004) Energy substrate modulates mitochondrial structure and oxidative capacity in cancer cells. *Cancer Res* **64:** 985–993

Sesaki H, Southard SM, Yaffe MP, Jensen RE (2003) Mgm1p, a dynamin-related GTPase, is essential for fusion of the mitochondrial outer membrane. *Mol Biol Cell* **14:** 2342–2356

Siegel MR, Sisler HD (1963) Inhibition of protein synthesis *in vitro* by cycloheximide. *Nature* **200:** 675–676

Skulachev VP (2001) Mitochondrial filaments and clusters as intracellular power-transmitting cables. *Trends Biochem Sci* **26:** 23–29

Smirnova E, Griparic L, Shurland DL, van der Bliek AM (2001) Dynamin-related protein Drp1 is required for mitochondrial division in mammalian cells. *Mol Biol Cell* **12:** 2245–2256

Soltys BJ, Gupta RS (1994) Changes in mitochondrial shape and distribution induced by ethacrynic acid and the transient formation of a mitochondrial reticulum. *J Cell Physiol* **159:** 281–294

Song Z, Chen H, Fiket M, Alexander C, Chan DC (2007) OPA1 processing controls mitochondrial fusion and is regulated by mRNA splicing, membrane potential, and Yme1L. *J Cell Biol* **178:** 749–755

Suen DF, Norris KL, Youle RJ (2008) Mitochondrial dynamics and apoptosis. *Genes Dev* **22:** 1577–1590

Sugioka R, Shimizu S, Tsujimoto Y (2004) Fzo1, a protein involved in mitochondrial fusion, inhibits apoptosis. *J Biol Chem* **279:** 52726–52734

Tavernarakis N, Driscoll M, Kyrpides NC (1999) The SPFH domain: implicated in regulating targeted protein turnover in stomatins and other membrane-associated proteins. *Trends Biochem Sci* **24:** 425–427

Twig G, Elorza A, Molina AJ, Mohamed H, Wikstrom JD, Walzer G, Stiles L, Haigh SE, Katz S, Las G, Alroy J, Wu M, Py BF, Yuan J, Deeney JT, Corkey BE, Shirihai OS (2008) Fission and selective fusion govern mitochondrial segregation and elimination by autophagy. *EMBO J* **27:** 433–446

Van Gestel K, Verbelen JP (2002) Giant mitochondria are a response to low oxygen pressure in cells of tobacco (Nicotiana tabacum L.). *J Exp Bot* **53:** 1215–1218

Wong ED, Wagner JA, Scott SV, Okreglak V, Holewinske TJ, Cassidy-Stone A, Nunnari J (2003) The intramitochondrial dynamin-related GTPase, Mgm1p, is a component of a protein complex that mediates mitochondrial fusion. *J Cell Biol* **160:** 303–311

Yoon Y, Krueger EW, Oswald BJ, McNiven MA (2003) The mitochondrial protein hFis1 regulates mitochondrial fission in mammalian cells through an interaction with the dynamin-like protein DLP1. *Mol Cell Biol* **23:** 5409–5420

Zuchner S, Mersiyanova IV, Muglia M, Bissar-Tadmouri N, Rochelle J, Dadali EL, Zappia M, Nelis E, Patitucci A, Senderek J, Parman Y, Evgrafov O, Jonghe PD, Takahashi Y, Tsuji S, Pericak-Vance MA, Quattrone A, Battaloglu E, Polyakov AV, Timmerman V *et al* (2004) Mutations in the mitochondrial GTPase mitofusin 2 cause Charcot-Marie-Tooth neuropathy type 2A. *Nat Genet* **36:** 449–451